Stability, Mixed Conductivity, and Thermomechanical Properties of Perovskite Materials for Fuel Cell Electrodes Based on $La_{0.5}A_{0.5}Mn_{0.5}Ti_{0.5}O_{3-\delta}$, $La_{0.5}Ba_{0.5}Ti_{0.5}Fe_{0.5}O_{3-\delta}$, and $(La_{0.5}A_{0.5})_{0.95}Cr_{0.5}Fe_{0.5}O_{3-\delta}$ (A = Ca, Ba)[1]

V. A. Kolotygin[a], *, E. V. Tsipis[a, b], M. V. Patrikeev[c], A. I. Ivanov[a], and V. V. Kharton[a, d]

[a]*Institute of Solid State Physics, Russian Academy of Sciences,*
ul. Akademika Osip'yana 2, Moscow oblast', Chernogolovka, 142432 Russia

[b]*Center for Mechanical Technology and Automation (TEMA), Faculty of Mechanical Engineering,*
University of Aveiro, Santiago Campus, 3810-193, Aveiro, Portugal

[c]*Institute of Solid-State Chemistry, Ural Branch, Russian Academy of Sciences,*
ul. Pervomaiskaya 91, Yekaterinburg, 620990 Russia

[d] *Center for Research in Ceramics and Composite Materials (CICECO), University of Aveiro,*
Santiago Campus, 3810-193, Aveiro, Portugal

*e-mail: kolotygin@issp.ac.ru
Received July 20, 2015

Abstract—For materials based on ferrites and manganites with Ca^{2+} and Ba^{2+} cations substituted into *A* sublattice, the functional properties are studied and the prospects as electrode materials for solid-oxide fuel cells are assessed. The electronic conductivity of materials based on $La_{0.5}A_{0.5}Mn_{0.5}Ti_{0.5}O_{3-\delta}$ is shown to decrease with the increase in the ionic radius of alkali-earth substituent; however, for $La_{0.5}Ba_{0.5}Mn_{0.5}Ti_{0.5}O_{3-\delta}$ and $La_{0.5}Ba_{0.5}Fe_{0.5}Ti_{0.5}O_{3-\delta}$, the appearance of *n*-conduction is observed during reduction, which may provide adequate conductivity under anodic conditions. Under the conditions of fuel cell operation, the thermal expansion coefficients of these materials are $(13.0-13.5) \times 10^{-6}$ K^{-1}. The thermal and chemical expansion increases with the increase in the radius of alkali-earth cation; the latter value does not exceed 0.2%, which is acceptable for preparation of electronic layers. The transition of oxygen through membranes based on materials studied is determined to the large extent by the kinetics of surface exchange which depends on the rate of delivery of oxygen vacancies to the surface. Doping of ferrites with chromium or titanium decreases the electronic and ionic conductivity; however, the presence of substituents in *B* sublattice makes it possible to stabilize the perovskite phase in a wide range of $p(O_2)$, decrease the thermal and chemical expansion, and prevent to the large extent the ordering of oxygen vacancies, which allows one to consider these materials as the candidates for electrodes in symmetrical solid-oxide fuel cells.

Keywords: perovskite, electronic conductivity, thermal expansion, chemical expansion, oxygen permeability, ionic conductivity, SOFC anode

DOI: 10.1134/S1023193516070089

INTRODUCTION

Recently, keen attention was drawn to symmetrical solid-oxide fuel cells (SOFC) with anode and cathode made of one and the same material [1−4]. The use of these systems makes it possible to minimize the number of components and, as a consequence, simplify and cheapen the technology of their preparation. Furthermore, the possibility of periodically alternating the oxidative and reductive media makes it possible to oxidize carbon- and/or sulfur-containing compounds formed when one uses natural gas and remove them

from the anode surface. However, the electrode materials used in SOFC should meet the requirements placed on both cathodic and anodic materials, i.e., exhibit phase and structural stability, adequate electronic-ionic conductivity, catalytic activity, and thermomechanical and chemical compatibility with the solid electrolyte under both oxidative and reductive conditions [2, 5, 6]. As the candidates for these electrodes, the perovskite and perovskite-like materials based on $(Ln, Sr)(Cr, Mn)O_{3-\delta}$ [7−12], $(La, A)(Cr, Mn)O_{3-\delta}$ (where A is the cation of an alkali-earth element) [13], $(La, Sr)(Cr, Fe)O_{3-\delta}$ [12, 14, 15], $(La, Sr)(Fe,Ti)O_{3-\delta}$ [16, 17], $La_{0.8}Sr_{0.2}Mn_{0.8}Sc_{0.2}O_{3-\delta}$ [18], $Sr(Fe, Mo)O_{3-\delta}$

---

[1] Published on the basis of the materials of III All-Russia Conference "Fuel Cells and Power Plants on Their Basis," Chernogolovka, 2015.

[19, 20], $La_{0.6}Sr_{1.4}MnO_{4-\delta}$ [21] were studied. In order to optimize the electrochemical properties of electrode materials, the relationship between their composition and functional properties was studied recently. In particular, for materials with the $(La, Sr)(Mn, Ti)O_{3-\delta}$ composition, the effect of the ratio of cations in the A [22, 23] and B sublattices [24, 25] on the stability, transport, and electrochemical properties was studied. It was noted that compositions with the manganese content no lower than 40−60% and the close contents of La and Sr are optimal for anodic materials. Perovskites of the series $(La, Sr)(Fe, Ti)O_{3-\delta}$ and $(La, Sr)(Cr, Fe)O_{3-\delta}$ and their derivatives were studied as the materials for membranes used for oxidizing hydrocarbons and also as the SOFC anodes [14, 16, 26−30]. It was noted that the increase in iron content provides the enhanced electronic and ionic conductivity and favors the catalytic activity, whereas doping with chromium/titanium stabilizes the perovskite structure in a wide range of $p(O_2)$, prevents the ordering processes, and lowers down the thermal and chemical expansion. Varying the ratios of cations in A and B sublattices made it possible to modify the electron transport in materials studied, particularly, shift the $p−n$ transition to the region of higher $p(O_2)$, thus providing the higher electronic conductivity under anodic conditions.

However, the largest part of these data were obtained on Sr-substituted perovskites, whereas the data on the effect on the nature of alkali-earth cations on the properties of materials are scarce [31−34]. On the other hand it is known that substitution of calcium for strontium can improve the phase stability of perovskites due to the close cationic radii of La^{3+} and Ca^{2+} [35], and also increase the electronic conductivity [13, 36], which is the crucial factor as regards the efficiency of perovskite anodes [2, 10, 13, 14, 36]. In particular, the authors of [13] demonstrated that the activity of cathodes and anodes of the $La_{0.7}A_{0.3}Cr_{0.5}Mn_{0.5}O_{3-\delta}$ composition increased in the series Ba < Sr < Ca. The observed tendency well agreed with the changes in the electronic conductivity of the corresponding materials under oxidative and reductive conditions.

On the other hand, besides providing high stability, the introduction of barium can increase the concentration of oxygen vacancies and the lattice free volume, which favors the higher ionic conductivity and also increases the electronic conductivity of the n-type [37−40]. Assuming that the phase and structural stability of perovskite materials, their transport and electrochemical properties may be improved by varying the cationic radius of the alkali-earth substituent, the present work is aimed at studying the functional properties of perovskite materials $La_{0.5}A_{0.5}Mn_{0.5}Ti_{0.5}O_{3-\delta}$, $La_{0.5}Ba_{0.5}Ti_{0.5}Fe_{0.5}O_{3-\delta}$, and $(La_{0.5}Ca_{0.5})_{0.95}Cr_{0.5}Fe_{0.5}O_{3-\delta}$ (A = Ca, Ba) and assessing their prospects as the electrodes in symmetrical SOFC.

EXPERIMENTAL

The studied materials were synthesized by the glycine-nitrate method, i.e., through oxidation of glycine by nitrates of corresponding metals. As the starting components, we used $La(NO_3)_3 \cdot 6H_2O$, $Mn(CH_3COO)_2 \cdot 4H_2O$, $Cr(NO_3)_3 \cdot 9H_2O$, $Fe(NO_3)_3 \cdot 9H_2O$, $Ba(NO_3)_2$, and $Ca(NO_3)_2 \cdot 4H_2O$. The required weights of these reagents were dissolved in water, after which glycine was added in one-and-a-half excess as compared with its stoichiometric amount. Water-nonsoluble TiO_2 (anatase) preliminarily annealed in air at 1173 K was added to the prepared solution, after which water was evaporated until spontaneous combustion. The resulting foam-like powder was annealed at 1073−1273 K for 2 h to remove organic components. To provide the complete reaction of TiO_2 with the other oxides, the reaction mixture was repeatedly annealed at 1473−1573 K; between annealings, the powder was crushed in a ball mill with zirconium-oxide balls.

To produce dense ceramic samples, we used uniaxial hydraulic pressing of powders under pressure of 80−100 MPa to form disks with the diameter of 20 mm and the thickness of 0.6−1.5 nm. Ceramics $La_{0.5}A_{0.5}Mn_{0.5}Ti_{0.5}O_{3-\delta}$ was sintered at 1773 K for 10 h and ceramics $La_{0.5}Ba_{0.5}Fe_{0.5}Ti_{0.5}O_{3-\delta}$ was sintered at 1728 K for 5 h. These conditions allowed single-phase gas-tight ceramics to be obtained. Sintering of perovskites $(La_{0.5}Ca_{0.5})_{0.95}Cr_{0.5}Fe_{0.5}O_{3-\delta}$ was carried out in the temperature range of 1223−1728 K.

To study the stability of materials under reductive conditions, the powders were annealed in a wet mixture of 10% H_2−90% N_2. The partial pressure of oxygen in the reactor was controlled by an oxygen sensor based on zirconium oxide. To study the chemical interaction between the tested materials and the zirconium electrolyte, disks were prepared from the mechanical mixture (50 : 50 mass %) of the tested oxide and $Zr_{0.85}Y_{0.15}O_{1.925}$ (8YSZ) by using uniaxial pressing under 50 MPa and then annealed at 1473−1573 K in air.

The phase composition of synthetic products and powders subjected to the above procedures was studied by the XRD method. The diffraction patterns were obtained by means of diffractometer Rigaku D/Max-B in CuK_α ($\lambda = 0.154178$ nm) radiation in the interval of angles $2\theta = 10°−80°$. The unit cell parameters of single-phase compositions or multiphase systems were calculated using the programs Fullprof or PowderCell.

For details of methods used for studying the transport and thermomechanical properties of materials, see [8, 10, 22, 27, 41]. Dilatometric measurements were carried out on ceramic samples shaped as parallelepipeds with the use of a vertical dilatometer Linseis L75/N1 calibrated on a cylindrical sample of Al_2O_3. To assess the thermal expansion, the experiments were carried out in air at the permanent heating to 1373 K and cooling at a rate of 3 K/min. Measurements of

Table 1. Unit cell parameters found for perovskites $La_{0.5}A_{0.5}Mn_{0.5}Ti_{0.5}O_{3-\delta}$ (A = Ca, Ba), $La_{0.5}Ba_{0.5}Fe_{0.5}Ti_{0.5}O_{3-\delta}$, and $(La_{0.5}Ca_{0.5})_{0.95}Fe_{0.5}Cr_{0.5}O_{3-\delta}$ after their annealing in air and in the flow of 10% $H_2-N_2-H_2O$ ($p(O_2) = (3-5) \times 10^{-17}$ atm) followed by slow cooling to room temperature

Composition	Synthetic conditions	Space group	a, nm	b, nm	c, nm	V, nm^3	Relative density, %
$La_{0.5}Ca_{0.5}Mn_{0.5}Ti_{0.5}O_{3-\delta}$	1573 K, air	$Pnma$	0.5467(2)	0.5478(2)	0.7754(2)	0.2322	91.1
	1223 K, $H_2-N_2-H_2O$	$Pnma$	0.5497(2)	0.5527(2)	0.7781(2)	0.2364	–
$La_{0.5}Ba_{0.5}Mn_{0.5}Ti_{0.5}O_{3-\delta}$	1573 K, air	$Pm\overline{3}m$	0.3960(2)	–	–	0.0621	84.1
	1223 K, $H_2-N_2-H_2O$	$Pm\overline{3}m$	0.3964(2)	–	–	0.0623	–
$La_{0.5}Ba_{0.5}Fe_{0.5}Ti_{0.5}O_{3-\delta}$	1423 K, air	$Pm\overline{3}m$	0.3962(2)	–	–	0.0622	83.8
	1223 K, $H_2-N_2-H_2O$	$Pm\overline{3}m$	0.3963(2)	–	–	0.0622	–
$(La_{0.5}Ca_{0.5})_{0.95}Fe_{0.5}Cr_{0.5}O_{3-\delta}$	1728, air	$Pnma$	0.5445(1)	0.7699(1)	0.5452(1)	0.2286	95.0

chemical expansion were carried out by two methods: by varying the temperature in the interval of 973–223 K in steps of 50 K at the fixed partial oxygen pressure and by changing the gas-medium composition under isothermal conditions. The oxygen activity in the gas phase was preset by the mixture $CO-CO_2$ prepared by passing CO_2 through the electrochemical pump. The partial pressure of oxygen in the gas mixture escaping from the dilatometer was determined by an electrochemical sensor.

The total specific conductivity of ceramic samples was measured by the four-probe method on direct current. The conductivity and the Seebeck coefficient were measured in air or in the gas mixture with controlled $p(O_2)$. In the latter case, a laboratory setup was used which was described in [27]. The oxygen permeability through gas-tight ceramic membranes [8, 10, 41] was measured on samples 1.00- and 0.60-mm thick. To assess the ionic conductivity and the kinetic constants of surface exchange, we used the model described in [41] which assumed proportionality between the rate of surface processes and the gradient of the oxygen chemical potential between the gas phase and the membrane surface.

RESULTS AND DISCUSSION

The materials of the $La_{0.5}A_{0.5}Mn_{0.5}Ti_{0.5}O_{3-\delta}$(A = Ca, Ba) and $La_{0.5}Ba_{0.5}Fe_{0.5}Ti_{0.5}O_{3-\delta}$ composition synthesized in air represented single-phase perovskites

(Figs. 1a–1c). Table 1 shows the space groups and lattice parameters. Insignificant deviations of structural parameters for Ba-substituted compositions were in good agreement with the closeness of ionic radii of Mn^{3+} and Fe^{3+} [35]. The reduction of $La_{0.5}Ca_{0.5}Mn_{0.5}Ti_{0.5}O_{3-\delta}$ produced a small amount of the MnO-based admixture, whereas $La_{0.5}Ba_{0.5}Mn_{0.5}Ti_{0.5}O_{3-\delta}$ and $La_{0.5}Ba_{0.5}Fe_{0.5}Ti_{0.5}O_{3-\delta}$ exhibited the high stability under both oxidative and reductive conditions (inserts in Figs. 1a–1c).

Figures 1d–1f show the diffraction patterns of powders synthesized by the contact annealing of perovskites together with 8YSZ. No foreign-phase reflexes were observed for the $La_{0.5}Ca_{0.5}Mn_{0.5}Ti_{0.5}O_{3-\delta}-$8YSZ system; however, it should be taken into account that the orthorhombic perovskite is characterized by a multitude of intrinsic peaks which can be overlapped by the peaks of possible reaction products. Despite the higher redox stability of the Ba-substituted analogue, its annealing in contact with 8YSZ produced peaks typical of the $BaZrO_3$ phase, which is well consistent with the high thermodynamic stability of the latter [42, 43]. On the other hand, no chemical interaction was observed between Ba-containing $La_{0.5}Ba_{0.5}Fe_{0.5}Ti_{0.5}O_{3-\delta}$ and YSZ (Fig. 1c). It deserves mention that the sufficiently high chemical compatibility with materials based on ZrO_2 was demonstrated by Ti-containing $La_{0.4}Sr_{0.6}Fe_{0.4}Ti_{0.6}O_{3-\delta}$ and $La_{0.4}Sr_{0.6}Mn_{0.6}Ti_{0.4}O_{3-\delta}$ with the close composition after their annealing together with the electrolyte in air at 1523 and 1673 K, respectively [24, 30].
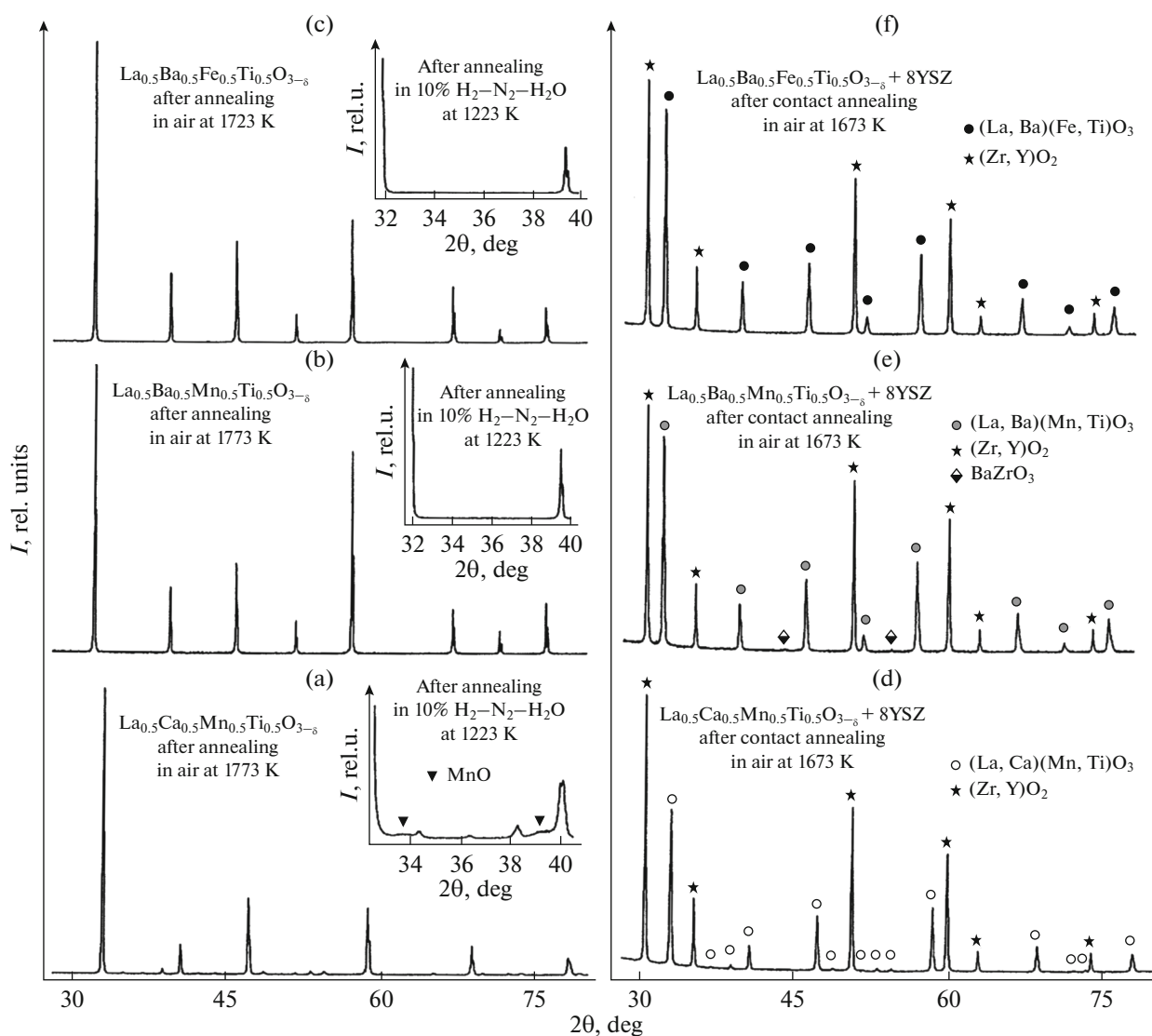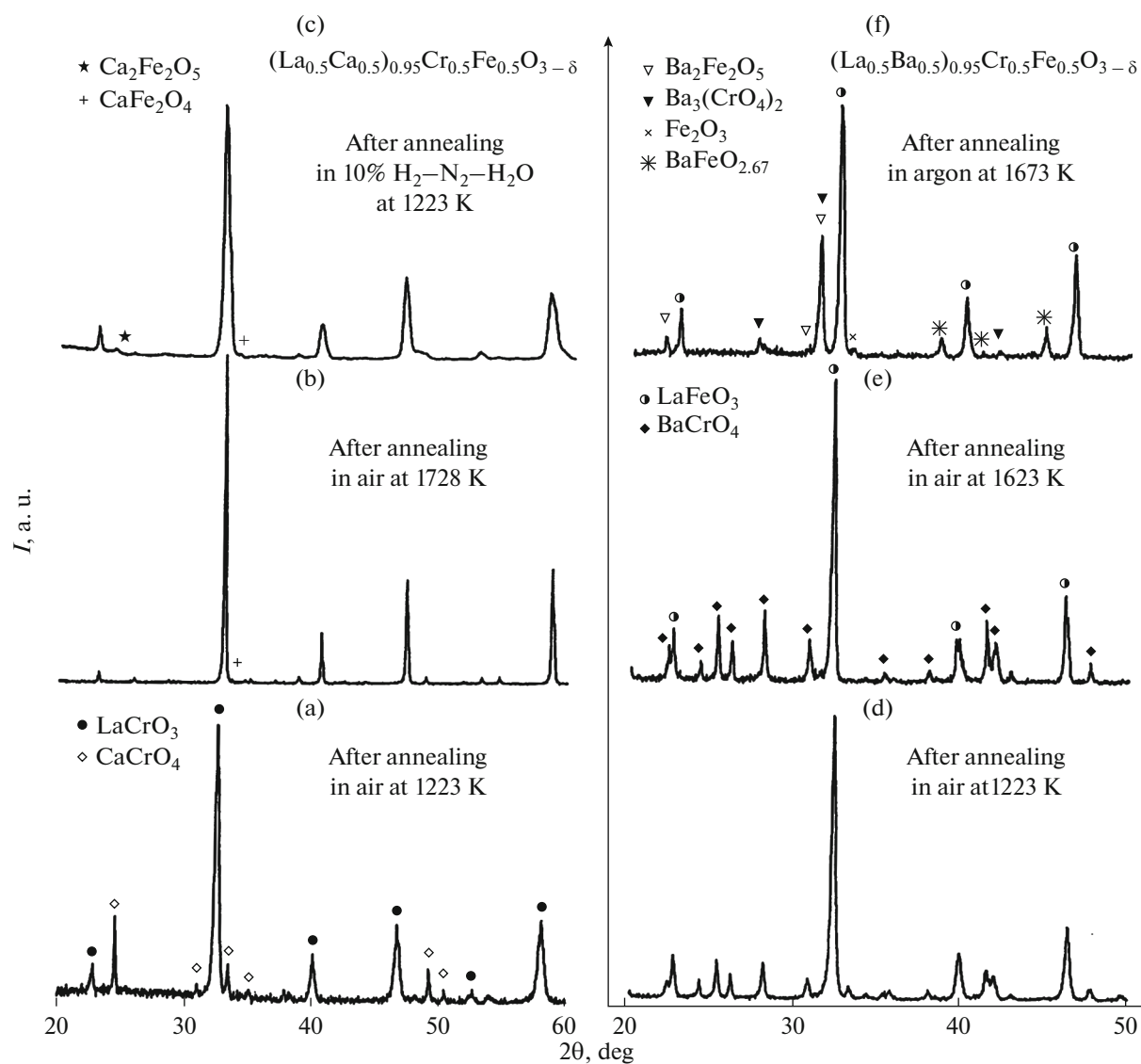
Fig. 1. Diffraction patterns of powders synthesized from ceramics (a) $La_{0.5}Ca_{0.5}Mn_{0.5}Ti_{0.5}O_{3-\delta}$, (b) $La_{0.5}Ba_{0.5}Mn_{0.5}Ti_{0.5}O_{3-\delta}$, (c) $La_{0.5}Ba_{0.5}Fe_{0.5}Ti_{0.5}O_{3-\delta}$ cooled slowly in air after annealing. Inserts show the diffraction patterns of the corresponding powders after their annealing at 1223 K in the atmosphere of 10% $H_2-N_2-H_2O$ ($p(O_2) = (3-5) \times 10^{-17}$ atm). Diffraction patterns of powders obtained after cosintering of (d) $La_{0.5}Ca_{0.5}Mn_{0.5}Ti_{0.5}O_{3-\delta}$, (e) $La_{0.5}Ba_{0.5}Mn_{0.5}Ti_{0.5}O_{3-\delta}$, and (f) $La_{0.5}Ba_{0.5}Fe_{0.5}Ti_{0.5}O_{3-\delta}$ together with 8YSZ at 1673 K in air.

Comparing the lattice parameters of the tested materials before and after their annealing together with 8YSZ (Table 2) revealed a certain increase in the unit cell volume of the perovskite phase with the increase in the annealing temperature. This effect may point to the presence of interdiffusion of cations between phases, particularly, to the insertion of large cations Zr^{4+} into the perovskite B-sublattice and the dissolution of transition-metal cations in the fluorite structure. Similar phenomena were reported at annealing of certain titanates together with zirconia-based phases [44–46]. This effect was observed to one or another extent for all Ti-containing perovskites

studied in the present work but was especially pronounced for $La_{0.5}Ba_{0.5}Mn_{0.5}Ti_{0.5}O_{3-\delta}$, in agreement with phase transitions after annealing.

The composition of the $(La_{0.5}Ca_{0.5})_{0.95}Cr_{0.5}Fe_{0.5}O_{3-\delta}$ solid solution after annealing at 1728 K in air was close to that of single-phase perovskite with the orthorhombic structure and an insignificant content of the $CaFe_2O_4$ phase (Fig. 2b). The reduction produced braunmillerite $Ca_2Fe_2O_5$ (Fig. 2c), which is typical of materials based on $CaFeO_3$ and $SrFeO_3$ [47–50]. It deserves mention that the literature data on the redox stability of materials based on (La, Sr)(Cr, Fe)O_3 are

Fig. 2. Diffraction patterns of powders $(La_{0.5}Ca_{0.5})_{0.95}Cr_{0.5}Fe_{0.5}O_{3-\delta}$ recorded (a) after the annealing in air at 1223 K, (b) after sintering of ceramics in air at 1728 K, (c) after annealing at 1223 K in $10\%H_2-N_2-H_2O$ ($p(O_2) = (3-5) \times 10^{-17}$ atm), which was followed by their cooling at the rate of 3 K/min. Diffraction patterns of $(La_{0.5}Ba_{0.5})_{0.95}Cr_{0.5}Fe_{0.5}O_{3-\delta}$ powders recorded (d) after annealing in air at 1223 K, (e) after sintering of ceramics in air at 1623 K, (f) after annealing at 1673 K in argon atmosphere ($p(O_2) = (8-10) \times 10^{-5}$ atm, which was followed by cooling at a rate of 3 K/min.

controversial [14, 26–28, 51, 52]; as a rule, the increase in the content of strontium and iron above 25 and 50%, respectively, leads to the formation of foreign phases under reductive conditions [26, 28, 52]. On the other hand, the content of admixtures in the tested $(La_{0.5}Ca_{0.5})_{0.95}Cr_{0.5}Fe_{0.5}O_{3-\delta}$ under both oxidative and reductive conditions was insignificant, which allows using this material as a component of the SOFC electrode.

The synthesis of $(La_{0.5}Ba_{0.5})_{0.95}Cr_{0.5}Fe_{0.5}O_{3-\delta}$ produced also the $BaCrO_4$ admixture the content of which could not be decreased by subsequent annealing (Figs. 2d, 2e). The high-temperature annealing of this material in the argon atmosphere reduced this admixture to $Ba_3(CrO_4)_2$ and also led to separation of an oxygen-deficient phase based on $BaFeO_{2.67}$ (Fig. 2f). The observed results point to insufficient solubility of barium in the perovskite lattice and agree with the high thermodynamic stability of barium chromate [13, 36]. Due to the complex phase composition and the high content of admixtures which could affect the electrochemical properties, no further investigations of $(La_{0.5}Ba_{0.5})_{0.95}Cr_{0.5}Fe_{0.5}O_{3-\delta}$ were carried out.

Table 2. Unit cell parameters of the perovskite phase found after the synthesis of materials $La_{0.5}Ca_{0.5}Mn_{0.5}Ti_{0.5}O_{3-\delta}$, $La_{0.5}Ba_{0.5}Mn_{0.5}Ti_{0.5}O_{3-\delta}$, and $La_{0.5}Ba_{0.5}Fe_{0.5}Ti_{0.5}O_{3-\delta}$ and also after their annealing together with 8YSZ at 1473 K and 1573 K in air

| Composition	Preparation conditions	Space group	a, nm	b, nm	c, nm
$La_{0.5}Ca_{0.5}Mn_{0.5}Ti_{0.5}O_{3-\delta}$	Original powder	$Pnma$	0.5467	0.5478	0.7754
	+8YSZ, annealing at 1473 K	$Pnma$	0.5478	0.5485	0.7737
	+8YSZ, annealing at 1573 K	$Pnma$	0.5481	0.5489	0.7742
$La_{0.5}Ba_{0.5}Mn_{0.5}Ti_{0.5}O_{3-\delta}$	Original powder	$Pm\bar{3}m$	0.3960	–	–
	+8YSZ, annealing at 1473 K	$Pm\bar{3}m$	0.3967	–	–
	+8YSZ, annealing at 1573 K	$Pm\bar{3}m$	0.3982	–	–
$La_{0.5}Ba_{0.5}Fe_{0.5}Ti_{0.5}O_{3-\delta}$	Original powder	$Pm\bar{3}m$	0.3962	–	–
	+8YSZ, annealing at 1473 K	$Pm\bar{3}m$	0.3964	–	–
	+8YSZ, annealing at 1573 K	$Pm\bar{3}m$	0.3966	–	–

Table 3. Activation energy of the specific conductivity in air and also of the oxygen flows through a dense membrane 1.00 mm thick on a single drop of partial oxygen pressure between the surfaces

Material	Specific conductivity		Oxygen flow	
	T, K	E_a, kJ/mol	T, K	E_a, kJ/mol
$La_{0.5}Ca_{0.5}Mn_{0.5}Ti_{0.5}O_{3-\delta}$	683–1253	26.5 ± 0.1	1223–1273	191 ± 42
	563–683	29.8 ± 3.8		
$La_{0.5}Ba_{0.5}Mn_{0.5}Ti_{0.5}O_{3-\delta}$	753–1273	31.9 ± 0.1	1173–1273	182 ± 31
	613–753	34.8 ± 1.7		
$La_{0.5}Ba_{0.5}Fe_{0.5}Ti_{0.5}O_{3-\delta}$	1053–1293	29.6 ± 1.0	1173–1273	189 ± 13
	653–1053	35.2 ± 0.5		
$(La_{0.5}Ca_{0.5})_{0.95}Fe_{0.5}Cr_{0.5}O_{3-\delta}$	1003–1273	22.0 ± 0.8	1023–1223	204 ± 2
	603–1003	27.4 ± 0.8		

All materials studied here exhibited the electronic conductivity which followed from the results of measurements of oxygen permeability which will be shown below. The conductivity was also of the thermally activated nature. For perovskites $La_{0.5}A_{0.5}Mn_{0.5}Ti_{0.5}O_{3-\delta}$, the conductivity decreased in the row Ca > Sr > Ba (Fig. 3); this tendency is typical of certain perovskites and can be associated with the weaker overlap of electron orbitals with the increase in the lattice volume [13, 36, 37]. Doping of ferrites $La_{0.5}Ba_{0.5}FeO_{3-\delta}$ and $La_{0.5}Ca_{0.5}FeO_{3-\delta}$ with titanium and chromium, respectively, led to a decrease in conductivity and an increase in the activation energy (Fig. 4, Table 3). On the other hand, for $(La_{0.5}Ca_{0.5})_{0.95}Fe_{0.5}Cr_{0.5}O_{3-\delta}$, the conductivity in air was 30–40 S/cm and did not degrade in time (Fig. 5), Hence, this composition can be considered as the potential cathode for SOFC.

Under changes in $p(O_2)$, the $La_{0.5}Ca_{0.5}Mn_{0.5}Ti_{0.5}O_{3-\delta}$ composition behaved like manganites do under moderate variations in the oxygen content [8, 22, 53]. Its conductivity changed insignificantly during initial reduction and then decreased due to the formation of a substantial number of oxygen vacancies and the decrease in the number of holes which served as charge carriers. At temperature below 1073 K, the changes in the oxygen nonstoichiometry were insignificant, which allowed the conductivity to remain at a constant level of 2–4 S/cm in a wide $p(O_2)$ interval including the anodic conditions (Fig. 3a). As a result of the more substantial oxygen losses, the reduction of $La_{0.5}Ba_{0.5}Mn_{0.5}Ti_{0.5}O_{3-\delta}$ led to the appearance of the n-type conductivity (Fig. 3b) typical of perovskites with the high content of both titanium and the donating substituent. In particular, the authors of [54, 55]
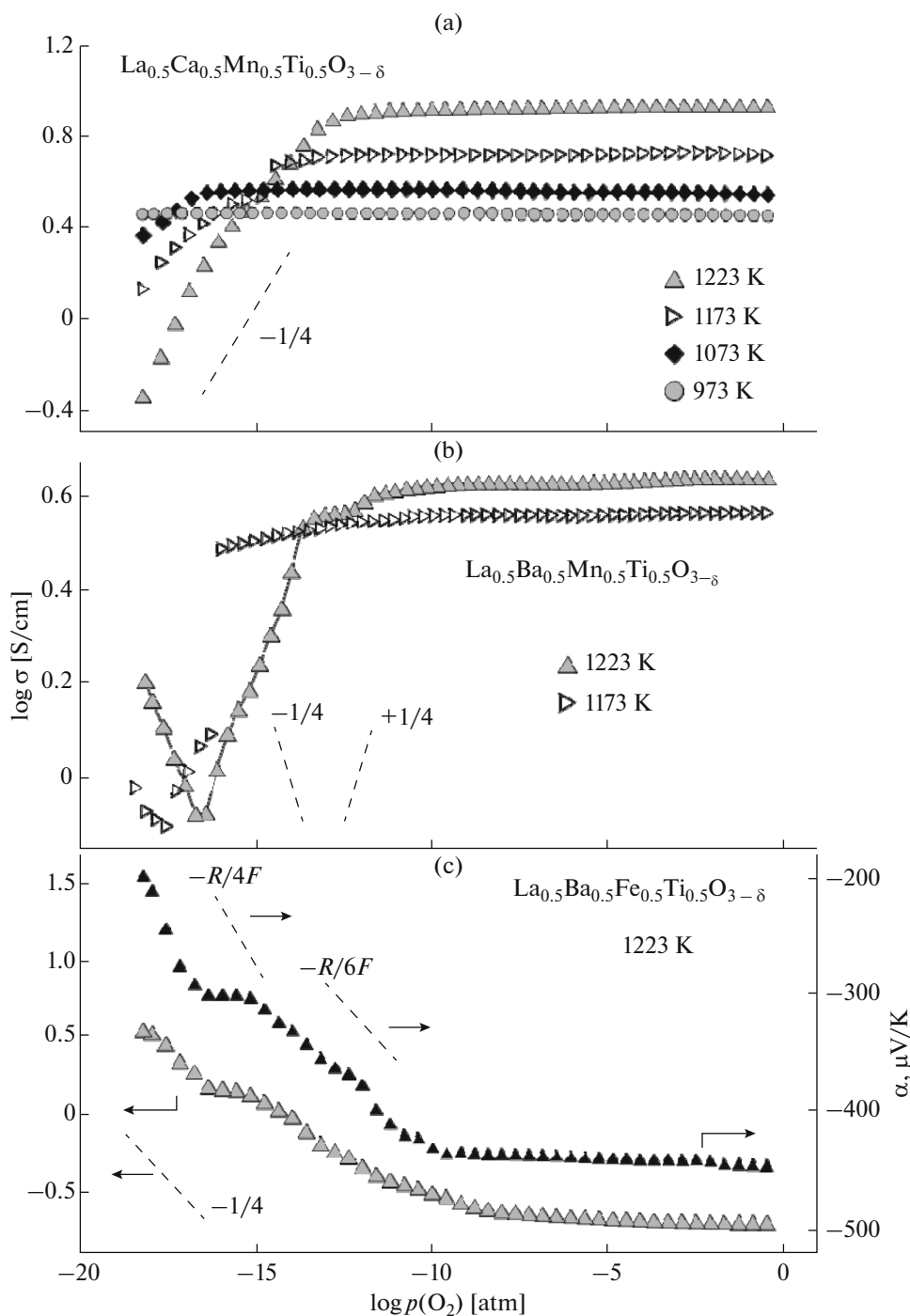
Fig. 3. Isotherms of specific conductivity and the Seebeck coefficient for ceramic samples of (a) $La_{0.5}Ca_{0.5}Mn_{0.5}Ti_{0.5}O_{3-\delta}$, (b) $La_{0.5}Ba_{0.5}Mn_{0.5}Ti_{0.5}O_{3-\delta}$, (c) $La_{0.5}Ba_{0.5}Fe_{0.5}Ti_{0.5}O_{3-\delta}$.

reported that oxides $(La,Ca)(Cr,Ti)O_{3-\delta}$ and $(La, Ba)(Cr, Ti)O_{3-\delta}$ can exhibit p-conduction in oxidative media and n-conduction in reductive media due to the presence of $Cr^{4+/3+}$ and $Ti^{4+/3+}$ redox pairs, respectively. The increase in the contents of La and Ti favors the reduction of Ti^{4+} and results in the shift of the $p-n$ transition to the region of high $p(O_2)$.

The higher level of oxygen nonstoichiometry of $La_{0.5}Ba_{0.5}Fe_{0.5}Ti_{0.5}O_{3-\delta}$ resulted in the shift of the $p-n$ transition to the still more oxidative region. As a result, the substantial contribution of n-type conductivity was observed at $p(O_2) < 10^{-10}$ atm (Fig. 3c), being characterized by the slope close to $-1/6$ and $-R/6F$ in the $\log\sigma$ vs. $\log p(O_2)$ and α vs. $\ln p(O_2)$ coordinates, respectively.
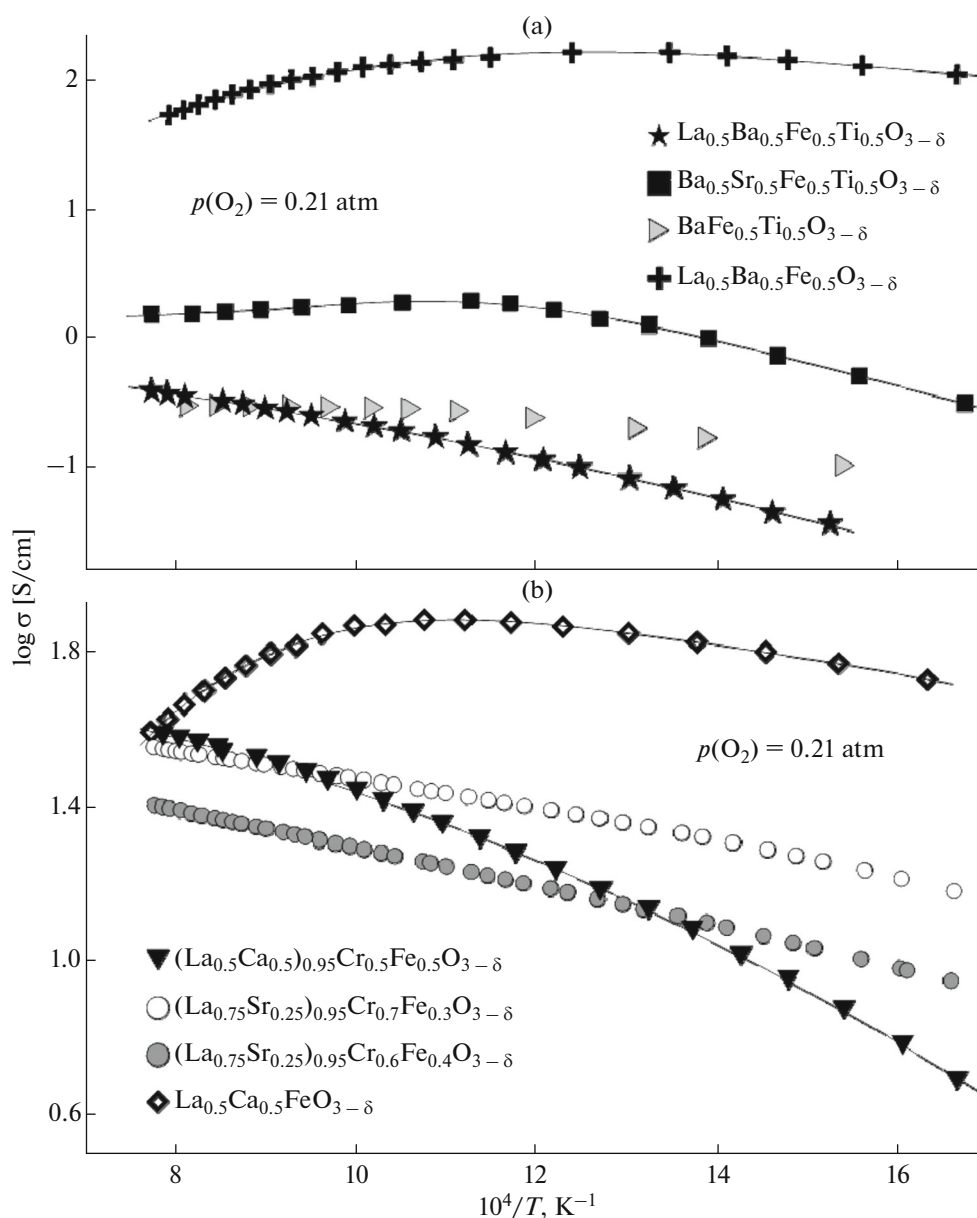
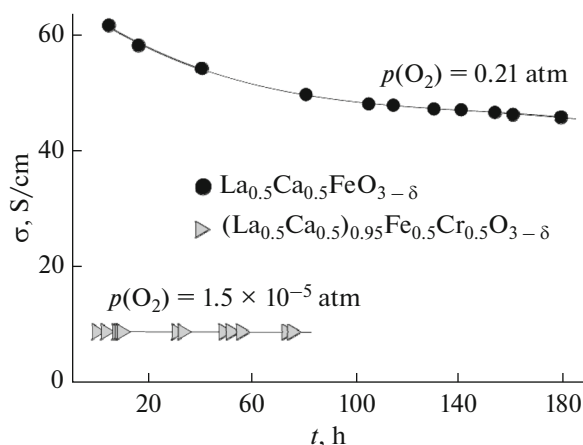**Fig. 4.** Temperature dependences of the specific conductivity of ceramic samples for (a) $La_{0.5}Ba_{0.5}Fe_{0.5}Ti_{0.5}O_{3-\delta}$ and (b) $(La_{0.5}Ca_{0.5})_{0.95}Cr_{0.5}Fe_{0.5}O_{3-\delta}$ in air. For a comparison, the results of [14, 37] are shown.

The further reduction led to the appearance of a plateau in the interval $p(O_2) \approx 10^{-16}$–10^{-15} atm; as $p(O_2)$ decreased further, the conductivity and the Seebeck coefficient continued to increase with the slope of $-1/4$ and $-R/4F$ in the aforementioned coordinates.

It should be mentioned that that at the reduction of $BaTi_{1-x}Mn_xO_{3-\delta}$, the slope of $\log n$ vs. $\log p(O_2)$ dependence, where n is the concentration of charge carriers of the n-type, is $-1/6$ in the region of high and low $p(O_2)$, increasing a little in the intermediate interval [56]. Such behavior was explained by the successive reduction of Mn^{4+} to Mn^{3+} and Mn^{2+}. Taking into account the principle of electroneutrality, the formation of Mn^{4+} or Fe^{4+} cations in perovskites $La_{0.5}Ba_{0.5}Mn_{0.5}Ti_{0.5}O_{3-\delta}$ and $La_{0.5}Ba_{0.5}Fe_{0.5}Ti_{0.5}O_{3-\delta}$ is possible in the presence of cationic vacancies and/or at disproportionation of Mn^{3+} and Fe^{3+} cations, respectively. On the other hand, the introduction of donating cations into titanates leads to the appearance of an interval in which the concentration of charge carriers is determined by the concentration of substituent, being practically independent of $p(O_2)$ [57]. The data obtained for $La_{0.5}Ba_{0.5}Fe_{0.5}Ti_{0.5}O_{3-\delta}$ make it possible to assume that the observed behavior is deter-

Fig. 5. Time dependences of the specific conductivity for $(La_{0.5}Ca_{0.5})_{0.95}Cr_{0.5}Fe_{0.5}O_{3-\delta}$ ($p(O_2) = 1.5 \times 10^{-5}$ atm) and $La_{0.5}Ca_{0.5}FeO_{3-\delta}$ ($p(O_2) = 0.21$ atm) at 1223 K.

mined by the redox interactions between cations $Fe^{4+/3+/2+}$ and $Ti^{4+/3+}$, and also oxygen and, probably, cationic vacancies. For the analysis of the defective structure, we need the information on nonstoichiometry of the materials involved; at the same time, it is also necessary to take into account certain kinetic factors capable of distorting the observed behavior. Irrespective of the mechanism of electron transfer in the tested materials, the acquired results suggest that the conductivity level of 5−10 S/cm can be achieved at the severe reduction of Ba-substituted $LaMn_{0.5}Ti_{0.5}O_{3-\delta}$ and $LaFe_{0.5}Ti_{0.5}O_{3-\delta}$, and also at the low-temperature kinetic stabilization of $La_{0.5}Ca_{0.5}Mn_{0.5}Ti_{0.5}O_{3-\delta}$.

The results of dilatometric measurements shown in Fig. 6 and Table 4 indicate that the increase in the cat-
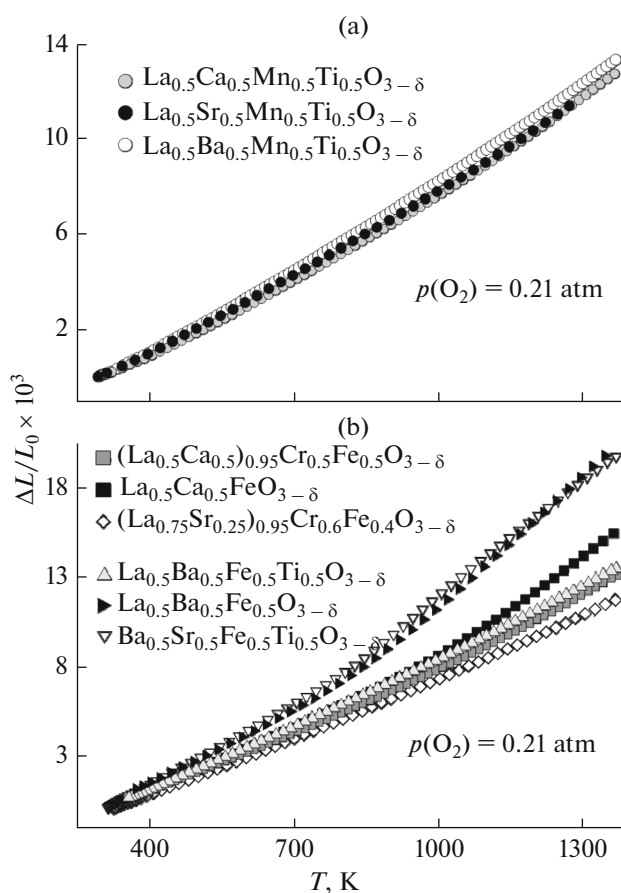
Fig. 6. Dilatometric curves measured in air for (a) $La_{0.5}A_{0.5}Mn_{0.5}Ti_{0.5}O_{3-\delta}$ (A = Ca, Ba) and also for (b) $La_{0.5}Ba_{0.5}Fe_{0.5}Ti_{0.5}O_{3-\delta}$ and $(La_{0.5}Ca_{0.5})_{0.95}Cr_{0.5}Fe_{0.5}O_{3-\delta}$ in the mode of permanent cooling at a rate of 3 K/min. For a comparison, the results of [14, 22, 37] are shown.

ionic radius of the dopant into A sublattice of $La_{0.5}A_{0.5}Mn_{0.5}Ti_{0.5}O_{3-\delta}$ leads to the increase in the thermal expansion coefficient (TEC) due to the larger unit cell volume and the substantial contribution made by the chemical component into the expansion for Ba-substituted materials (Table 5). On the other hand, in the temperature range of SOFC operation, the TEC values do not exceed $(13.0-13.5)\,10^{-6}\,K^{-1}$, whereas the chemical expansion is 0.1−0.2%, lying at the boundary of the acceptable range that ensures thermomechanical compatibility of the electrode with the other SOFC components [57, 58].

Figure 7 shows the results of measuring the chemical expansion under isothermal conditions for certain perovskites based on $La_{1-x}A_xFeO_3$. For undoped ferrites, the volume variations pass through the maximum at $p(O_2) \approx 10^{-4}-10^{-6}$ atm due to the formation of domains with the ordered structure in the perovskite lattice [47−50]. Despite the substantially lower extent

Table 4. Thermal expansion coefficients of ceramic samples of $La_{0.5}A_{0.5}Mn_{0.5}Ti_{0.5}O_{3-\delta}$ (A = Ca, Ba), $La_{0.5}Ba_{0.5}Fe_{0.5}Ti_{0.5}O_{3-\delta}$, and $(La_{0.5}Ca_{0.5})_{0.95}Fe_{0.5}Cr_{0.5}O_{3-\delta}$ in air

Material	T, K	$TEC \times 10^6$, K^{-1}
$La_{0.5}Ca_{0.5}Mn_{0.5}Ti_{0.5}O_{3-\delta}$	303−923	10.69 ± 0.01
	923−1223	13.01 ± 0.02
	1223−1373	14.04 ± 0.06
$La_{0.5}Ba_{0.5}Mn_{0.5}Ti_{0.5}O_{3-\delta}$	303−923	11.39 ± 0.07
	923−1223	13.33 ± 0.02
	1223−1373	14.33 ± 0.03
$La_{0.5}Ba_{0.5}Fe_{0.5}Ti_{0.5}O_{3-\delta}$	303−923	11.82 ± 0.01
	923−1223	13.26 ± 0.01
	1223−1373	14.11 ± 0.02
$(La_{0.5}Ca_{0.5})_{0.95}Fe_{0.5}Cr_{0.5}O_{3-\delta}$	303−923	10.87 ± 0.01
	923−1223	13.30 ± 0.03
	1223−1373	15.20 ± 0.02

of expansion, the similar behavior was observed for $La_{0.5}Ba_{0.5}Fe_{0.5}Ti_{0.5}O_{3-\delta}$, which allows one to assume certain ordering in the material studied, although the XRD data and the results of measuring the total conductivity do not allow us to give unambiguous answer as regards the structural changes. The analogous structural behavior was observed earlier for certain titanium-doped ferrites [33, 59]. Yet another reason for the observed maximum can be associated with the action of the CO/CO_2 atmosphere on the Ba-containing materials, which may induce the formation of an insignificant amount of impurity phases in concentrations below the XRD detection limit and also affect the reduction mechanism and, hence, its kinetics. It deserves mention that at the subsequent equilibration of the material in argon, the length of the sample was partially recovered despite the appearance of a large hysteresis.

Irrespective of the above processes, the presence of chromium or titanium in $La_{0.5}Ca_{0.5}FeO_{3-\delta}$ or $La_{0.5}Ba_{0.5}FeO_{3-\delta}$ substantially decreased their thermal and chemical expansion (Figs. 6b, 7); the TEC of materials studied in the temperature range of SOFC functioning was 13.3×10^{-6} K^{-1}, whereas the maximum linear change in the size of $La_{0.5}Ba_{0.5}Fe_{0.5}Ti_{0.5}O_{3-\delta}$ ceramics on isothermal redox cycling did not exceed 0.015%. Somewhat larger changes (0.02−0.03%) were observed when the chemical expansion was measured by yet another method which consisted of measuring deviations in the relative elongation values at thermal cycling of samples in various gas atmospheres (Table 5). The reason for these deviations can be associated with some kinetic factors as well as with the lower final $p(O_2)$ in the latter case.

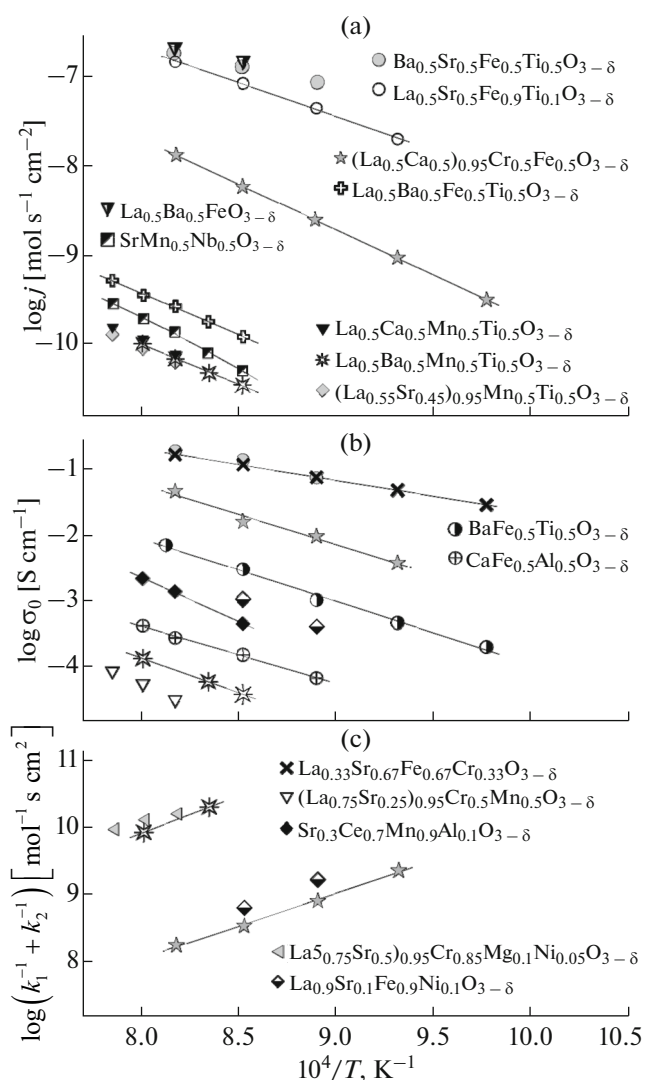Figure 8a shows some examples of the temperature dependences of oxygen flows for materials tested.
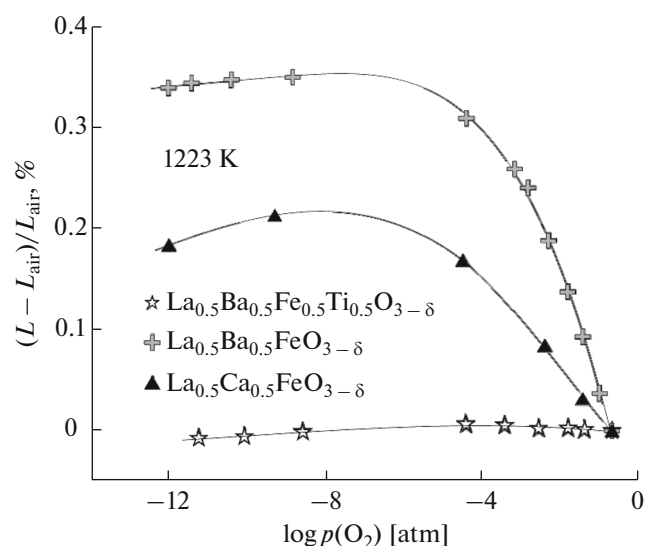
Fig. 7. Isothermal dependences of the changes in the length of ceramic samples based on $La_{0.5}Ba_{0.5}Fe_{0.5}Ti_{0.5}O_{3-\delta}$, $La_{0.5}Ba_{0.5}FeO_{3-\delta}$, and $La_{0.5}Ca_{0.5}FeO_{3-\delta}$ with respect to their initial length in air on the partial oxygen pressure.

Materials based on $La_{0.5}A_{0.5}Mn_{0.5}Ti_{0.5}O_{3-\delta}$ exhibited the close levels of flows regardless of the cation radius. The weak effect of the cationic composition in the A sublattice on the ion transfer was also reported for $(La, Sr)(Mn, Cr, Ti)O_{3-\delta}$ and $(La, Sr)(Mn, Ti)O_{3-\delta}$ perovskites [10, 22]. On the other hand, the higher level of permeability was observed $La_{0.5}Ba_{0.5}Fe_{0.5}Ti_{0.5}O_{3-\delta}$, which points to the enhanced concentration of oxygen vacancies involved in the ion-transfer and surface processes. This assumption is consistent with the substantial contribution of the n-type conductivity for the latter composition (Fig. 3c).

Table 5. Change in the relative elongation of ceramics $La_{0.5}A_{0.5}Mn_{0.5}Ti_{0.5}O_{3-\delta}$ (A = Ca, Ba) and $La_{0.5}Ba_{0.5}Fe_{0.5}Ti_{0.5}O_{3-\delta}$ at isothermal reduction in the mixture $CO-CO_2$ ($p(O_2) = 10^{-21}-10^{-15}$ atm)

T, K	$(L - L_{air})/L_{air} \times 10^3$		
	$La_{0.5}Ca_{0.5}Mn_{0.5}Ti_{0.5}O_{3-\delta}$	$La_{0.5}Ba_{0.5}Mn_{0.5}Ti_{0.5}O_{3-\delta}$	$La_{0.5}Ba_{0.5}Fe_{0.5}Ti_{0.5}O_{3-\delta}$
1223	0.74	1.76	−0.26
1173	0.72	1.77	−0.28
1123	0.73	1.80	−0.25
1073	0.74	1.90	−0.31
1023	0.76	2.00	−0.32
973	0.82	2.00	−0.32

Fig. 8. (a) Temperature dependences of the specific oxygen flow through gas-tight membranes ($d = 1.00$ mm) at the fixed drop of partial oxygen pressure $p_2/p_1 = 1.0$. Temperature dependences of (b) ionic conductivity and (c) the sum of reciprocal constants of surface exchange, calculated in the framework of a model described in [41], at $p(O_2) = 0.21$ atm. For a comparison, the results of [8, 22, 27, 41, 60–62] are shown.


Fig. 9. Isothermal dependences of (a, c) specific oxygen flow and (b) specific oxygen permeability through gas-tight membranes of (a, b) $La_{0.5}Ba_{0.5}Mn_{0.5}Ti_{0.5}O_{3-\delta}$ and (c) $(La_{0.5}Ca_{0.5})_{0.95}Cr_{0.5}Fe_{0.5}O_{3-\delta}$ with the thickness of 1.00 mm and 0.60 mm. The partial oxygen pressure on the fed side of the membrane (p_2) is 0.21 atm.

The decrease in the thickness of a membrane based on $La_{0.5}Ba_{0.5}Mn_{0.5}Ti_{0.5}O_{3-\delta}$ leads to an increase the oxygen flow through the membrane and a decrease in the corresponding specific oxygen permeability (Figs. 9a, 9b). Such behavior suggests the comparable contributions by the limiting stages associated with the bulk diffusion of oxygen and the surface effects. To assess quantitatively the above processes, we used the model described in [41, 60]; the results of calculations are shown in Figs. 8b, 8c, and 10. The ionic conductivity of $La_{0.5}Ba_{0.5}Mn_{0.5}Ti_{0.5}O_{3-\delta}$ was 10^{-4} S/cm and somewhat increased with the increase in the gradient

of partial oxygen pressure through the membrane (Fig. 10a) due to the formation of oxygen vacancies on reduction.

According to Fig. 9c, the decrease in the thickness of the $(La_{0.5}Ca_{0.5})_{0.95}Cr_{0.5}Fe_{0.5}O_{3-\delta}$ membrane from 1.0 to 0.6 mm affects only weakly the oxygen flows through membrane, which suggests the relatively slow surface kinetics. The ionic conductivity of the material was 10^{-2} S/cm, which allowed for the extension of the zone of electrochemical processes on SOFC electrodes; however, account should be taken on the large error of determination of this parameter due to the closeness of flows for membranes with different thickness.

Figures 8b and 8c compare the temperature dependences of the ionic conductivity and the sum of recipro-
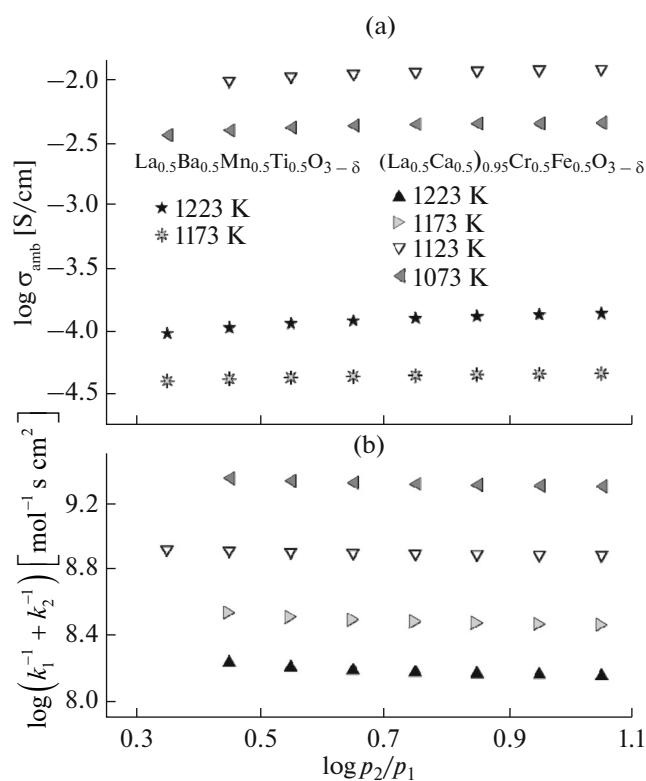
Fig. 10. Isothermal dependences of (a) conductivity and (b) the sum of reciprocal constants of surface exchange found within the framework of a model described in [41] on the drop of partial oxygen pressure for ceramic membranes (a) $La_{0.5}Ba_{0.5}Mn_{0.5}Ti_{0.5}O_{3-\delta}$ and (a, b) $(La_{0.5}Ca_{0.5})_{0.95}Cr_{0.5}Fe_{0.5}O_{3-\delta}$.

cal rate constants of surface exchange for materials under study with the literature data [8, 22, 27, 41, 60−62]. The corresponding activation energies are close to one another for both $La_{0.5}Ba_{0.5}Mn_{0.5}Ti_{0.5}O_{3-\delta}$ and $(La_{0.5}Ca_{0.5})_{0.95}Cr_{0.5}Fe_{0.5}O_{3-\delta}$ (210 an 185 kJ/mol, respectively), which suggests the substantial role played by ionic diffusion in the surface processes of both materials. Like the total conductivity, the ionic conductivity of $(La_{0.5}Ca_{0.5})_{0.95}Cr_{0.5}Fe_{0.5}O_{3-\delta}$ is somewhat lower as compared with certain other ferrites; however, moderate substitution of chromium for iron makes it possible to stabilize to a certain extent the perovskite phase and also decrease the TEC to the acceptable level. Thus, the materials of the $(La_{0.5}Ca_{0.5})_{0.95}Cr_{0.5}Fe_{0.5}O_{3-\delta}$ composition can serve as electrodes in symmetrical SOFC.

CONCLUSIONS

Perovskites with the composition of $La_{0.5}Ca_{0.5}Mn_{0.5}Ti_{0.5}O_{3-\delta}$, $La_{0.5}Ba_{0.5}Mn_{0.5}Ti_{0.5}O_{3-\delta}$, $La_{0.5}Ba_{0.5}Fe_{0.5}Ti_{0.5}O_{3-\delta}$, and $(La_{0.5}Ca_{0.5})_{0.95}Cr_{0.5}Fe_{0.5}O_{3-\delta}$ exhibit sufficient phase stability under oxidative and reductive conditions. $La_{0.5}Ca_{0.5}Mn_{0.5}Ti_{0.5}O_{3-\delta}$ and $La_{0.5}Ba_{0.5}Fe_{0.5}Ti_{0.5}O_{3-\delta}$ are chemically inactive with respect to the 8YSZ solid electrolyte up to 1673 K, although certain changes in unit cell parameters point to the interdiffusion of cations between phases. The joint annealing of $La_{0.5}Ba_{0.5}Mn_{0.5}Ti_{0.5}O_{3-\delta}$ with 8YSZ leads to the formation of the $BaZrO_3$, which can affect the efficiency and the service life of the corresponding electrochemical cell. As regard its total conductivity, $La_{0.5}Ca_{0.5}Mn_{0.5}Ti_{0.5}O_{3-\delta}$ exhibits the properties typical of the electronic conductor of the *p*-type, whereas for Ba-substituted perovskites, a substantial contribution of *n*-conductivity is observed under reductive conditions. The conductivity of $La_{0.5}Ba_{0.5}Mn_{0.5}Ti_{0.5}O_{3-\delta}$ and $La_{0.5}Ba_{0.5}Fe_{0.5}Ti_{0.5}O_{3-\delta}$ at 1223 K, and also of $La_{0.5}Ca_{0.5}Mn_{0.5}Ti_{0.5}O_{3-\delta}$ under the conditions of low-temperature stabilization in the reductive media amounts to 3−5 S/cm. The TEC of materials in the working zone of SOFC is $(13.0-13.5)\times 10^{-6}$ K^{-1}. The linear chemical expansion under isothermal conditions increases with the increase in the ionic radius of the dopant into the perozskite *A* sublattice but does not exceed 0.2%. The oxygen permeability of membranes is substantially limited by surface effects which, in turn, are determined by the diffusion rate of oxygen vacancies to the surface. The results acquired point to the possibility of using these perovskites as the electrodes in symmetrical SOFC, provided their electronic conductivity under reductive conditions can be made higher. The additional advantage of the material based on $(La_{0.5}Ca_{0.5})_{0.95}Cr_{0.5}Fe_{0.5}O_{3-\delta}$ is its relatively high ionic conductivity equal to $\sim 10^{-2}$ S/cm, which may favor the extension of the zone of occurrence of electrochemical processes.

REFERENCES

1. Ruiz-Morales, J.C., Marrero-Lopes, D., Canales-Vazquez, J., and Irvine, J.T.S., *RSC Adv.,* 2011, vol. 1, p. 1403.

2. Kharton, V.V., *Solid State Electrochemistry II: Electrodes, Interfaces and Ceramic Membranes,* Weinheim: Wiley-VCH, 2011.

3. Zhang, P., Guan, G., Khaerudini, D.S., Hao, X., Xue, C., Han, M., Kasai, Y., and Abudula, A., *J. Power Sources*, 2015, vol. 276, p. 347.

4. El Himri, A., Marrero-Lopez, D., Ruiz-Morales, J.C., Pena-Martinez, J., and Nunez, P., *J. Power Sources,* 2009, vol. 188, p. 230.

5. Goodenough, J.B. and Huang, Y.B., *J. Power Sources,* 2007, vol. 173, p. 1.

6. Jiang, S.P. and Chan, S.H., *J. Mater. Sci.,* 2004, vol. 39, p. 4405.

7. Tao, S. and Irvine, J.T.S., *J. Electrochem. Soc.,* 2004, vol. 151, p. A252.

8. Kharton, V.V., Tsipis, E.V., Marozau, I.P., Viskup, A.P., Frade, J.R., and Irvine, J.T.S., *Solid State Ionics,* 2007, vol. 178, p. 101.

9. Delahaye, T., Jardiel, T., Joubert, O., Laucournet, R., Gauthier, G., and Caldes, M.T., *Solid State Ionics,* 2011, vol. 184, p. 39.

10. Kolotygin, V.A., Tsipis, E.V., Shaula, A.L., Naumovich, E.N., Frade, J.R., Bredikhin, S.I., and Kharton, V.V., *J. Solid-State Electrochem.*, 2011, vol. 15, p. 313.

11. Jiang, S.P., Zhang, L., and Zhang, Y., *J. Mater. Chem.,* 2007, vol. 17, p. 2627.

12. Pena-Martinez, J., Marrero-Lopez, D., Perez-Coll, D., Ruiz-Morales, J.C., and Nunez, P., *Electrochim. Acta,* 2007, vol. 52, p. 2950.

13. Zhang, L., Chen, X.B., Jiang, S.P., He, H.Q., and Xiang, Y., *Solid State Ionics,* 2009, vol. 180, p. 1076.

14. Lu, M.F., Tsipis, E.V., Waerenborgh, J.C., Yaremchenko, A.A., Kolotygin, V.A., Bredikhin, S.I., and Kharton, V.V., *J. Power Sources,* 2012, vol. 206, p. 59.

15. Chen, M., Paulson, S., Thangadurai, V., and Birss, V., *J. Power Sources,* 2013, vol. 236, p. 68.

16. Canales-Vazquez, J., Ruiz-Morales, J.C., Marrero-Lopez, D., Pena-Martinez, J., Nunes, P., and Gomez-Romero, P., *J. Power Sources,* 2007, vol. 171, p. 552.

17. Ruiz-Morales, J.C., Canales-Vazquez, J., Lincke, H., Pena-Martinez, J., Marrero-Lopez, D., Perez-Coll, D., Irvine, J.T.S., and Nunez, P., *Boll. Soc. Esp. Ceram. Vidrio,* 2008, vol. 47, p. 183.

18. Zheng, Y., Zhang, C., Ran, R., Cai, R., Shao, Z., and Farrusseng, D., *Acta Mater.,* 2009, vol. 57, p. 1165.

19. Fernandez-Ropero, A.J., Porras-Vazquez, J.M., Cabeza, A., Slater, P.R., Marrero-Lopez, D., and Losilla, E.R., *J. Power Sources,* 2014, vol. 249, p. 405.

20. Meng, X., Liu, X., Han, D., Wu, H., Li, J., and Zhan, Z., *J. Power Sources,* 2014, vol. 252, p. 58.

21. Zhou, J., Chen, G., Wu, K., and Cheng, Y., *J. Power Sources,* 2014, vol. 270, p. 418.

22. Kolotygin, V.A., Tsipis, E.V., Ivanov, A.I., Fedotov, Y.S., Burmistrov, I.N., Agarkov, D.A., Sinitsyn, V.V., Bredikhin, S.I., and Kharton, V.V., *J. Solid-State Electrochem.,* 2012, vol. 16, p. 2335.

23. Ivanov, A.I., Agarkov, D.A., Burmistrov, I.N., Kudrenko, E.A., Bredikhin, S.I., and Kharton, V.V., *Russ. J. Electrochem.,* 2014, vol. 50, p. 730.

24. Fu, Q.X., Tietz, F., and Stover, D., *J. Electrochem. Soc.,* 2006, vol. 153, p. 74.

25. Corre, G., Kim, G., Cassidy, M., Vohs, J.M., Gorte, R.J., and Irvine, J.T.S., *Chem. Mater.,* 2009, vol. 21, p. 1077.

26. Tao, S. and Irvine, J.T.S., *Chem. Mater.,* 2004, vol. 16, p. 4116.

27. Kozhevnikov, V.L., Leonidov, I.A., Bahteeva, J.A., Patrakeev, M.V., Mitberg, E.B., and Poeppelmeier, K.R., *Chem. Mater.,* 2004, vol. 16, p. 5014.

28. Haag, J.M., Barnett, S.A., Richardson, Jr.J.W., and Poeppelmeier, K.R., *Chem. Mater.,* 2010, vol. 22, p. 3283.

29. Park, C.Y., Huang, D.X., Jacobson, A.J., Hu, L., and Mims, C.A., *Solid State Ionics,* 2006, vol. 177, p. 2227.

30. Fagg, D.P., Kharton, V.V., Kovalevsky, A.V., Viskup, A.P., Naumovich, E.N., and Frade, J.R., *J. Eur. Ceram. Soc.,* 2001, vol. 21, p. 1831.

31. Hosseini, N.R., Sammes, N.M., and Chung, J.Sh., *J. Power Sources,* 2014, vol. 245, p. 599.

32. Molero-Sanchez, B., Prado-Gonjal, J., Avila-Brande, D., Chen, M., Moran, E., and Birss, V., *Int. J. Hydrogen Energy,* 2015, vol. 40, p. 1902.

33. Dunyushkina, L.A., Gorbunov, V.A., Babkina, A.A., and Esina, N.O., *Ionics,* 2003, vol. 9, p. 67.

34. Azad, A.K., Eriksson, G.G., and Irvine, J.T.S., *Mater. Res. Bull.,* 2009, vol. 44, p. 1451.

35. Shannon, R.D., *Acta. Crystal.,* 1976, vol. A32, p. 751.

36. Jiang, S.P., Liu, L., Wong, K.P., Wu, P., Li, J., and Pu, J., *J. Power Sources,* 2008, vol. 176, p. 82.

37. Kharton, V.V., Kovalevsky, A.A., Patrakeev, M.V., Tsipis, E.V., Viskup, A.P., Kolotygin, V.V., Yaremchenko, A.A., Shaula, A.L., Kiselev, E.A., and Waerenborgh, J.C., *Chem. Mater.,* 2008, vol. 20, p. 6457.

38. Serra, J.M., Vert, V.B., Betz, M., Haanappel, V.A.C., Meulenberg, W.A., and Tietz, F., *J. Electrochem. Soc.,* 2008, vol. 155, p. B207.

39. Baumann, F.S., Fleig, J., Cristiani, G., Stuhlhofer, B., Habermeier, H.U., and Maier, J., *J. Electrochem. Soc.,* 2007, vol. 154, p. B913.

40. Shao, Z.P., Yang, W.S., Cong, Y., Dong, H., Tong, J.H., and Xiong, G.X., J. Membr. Sci., 2000, vol. 172 P, p. 177.

41. Marozau, I.P., Kharton, V.V., Viskup, A.P., Frade, J.R., and Samakhval, V.V., *J. Eur. Ceram. Soc.,* 2006, vol. 26, p. 1371.

42. Matsui, T., *Thermochim. Acta,* 1995, vol. 253, p. 155.

43. Kreuer, K.D., Adams, St., Munch, W., Fuchs, A., Klock, U., and Maier, J., *Solid State Ionics,* 2001, vol. 145, p. 295.

44. Chen, G., Kishimoto, H., Yamaji, K., Kuramoto, K., and Horita, T., *J. Electrochem. Soc.,* 2015, vol. 162, p. F223.

45. Burnat, D., Heel, A., Holzer, L., Otal, E., Kata, D., and Graule, T., *Int. J. Hydrogen Energy,* 2012, vol. 37, p. 18326.

46. Ma, Q., Tietz, F., Sebold, D., and Stover, D., *J. Power Sources,* 2010, vol. 195, p. 1920.

47. Hagenmuller, P., Pouchard, M., and Grenier, J.C., *Solid State Ionics,* 1990, vol. 43, p. 7.

48. Nemudry, A., Weiss, M., Gainutdinov, I., Boldyrev, V., and Schollhorn, R., *Chem. Mater.,* 1998, vol. 10, p. 2403.

49. Berastegui, P., Eriksson, S.G., and Hull, S., *Mater. Res. Bull.,* 1999, vol. 34, p. 303.

50. Patrakeev, M.V., Bahteeva, J.A., Mitberg, E.B., Leonidov, I.A., Kozhevnikov, V.L., and Poeppelmeier, K.R., *J. Solid State Chem.,* 2003, vol. 172, p. 219.

51. Sfeir, J., *J. Power Sources,* 2003, vol. 118, p. 276.

52. Oishi, M., Yashiro, K., Sato, K., Mizusaki, J., and Kawada, T., *J. Solid State Chem.,* 2008, vol. 181, p. 3177.

53. Mizusaki, J., Yonemura, Y., Kamata, H., Ohyama, K., Mori, N., Takai, H., Tagawa, H., Dokiya, M., Naraya, K., Sasamoto, T., Inaba, H., and Hashimoto, T., *Solid State Ionics,* 2000, vol. 132, p. 167.

54. Vashook, V., Vasylechko, L., Zosel, J., Muller, R., Ahlborn, E., and Guth, U., *Solid State Ionics,* 2004, vol. 175, p. 151.

55. Karen, P. and Norby, T., *J. Electrochem. Soc.,* 1998, vol. 145, p. 264.

56. Kim, J.Y., Song, C.R., and Yoo, H.I., *J. Electroceram.,* 1997, vol. 1, p. 27.

57. Fu, Q.X. and Tietz, F., *Fuel Cells,* 2008, vol. 8, p. 283.

58. Sarantaridis, D. and Atkinson, A., *Fuel Cells,* 2007, vol. 7, p. 246.

59. Steinsvik, S., Bugge, R., Gjonnes, J., Tafto, J., and Norby, T., *J. Phys. Chem. Solids,* 1997, vol. 58, p. 969.

60. Tsipis, E.V., Kiselev, E.A., Kolotygin, V.A., Waerenborgh, J.C., Cherepanov, V.A., and Kharton, V.V., *Solid State Ionics,* 2009, vol. 179, p. 2170.

61. Tsipis, E.V., Patrakeev, M.V., Kharton, V.V., Yaremchenko, A.A., Mather, G.C., Shaula, A.L., Leonidov, I.A., Kozhevnikov, V.L., and Frade, J.R., *Solid State Sci.,* 2005, vol. 7, p. 355.

62. Kharton, V.V., Marozau, I.P., Vyshatko, N.P., Shaula, A.L., Viskup, A.P., Naumovich, E.N., and Marques, F.M.B., *Mater. Res. Bull.,* 2003, vol. 38, p. 773.

Translated by T.Ya. Safonova